

SCIENTIFIC REPORTS



OPEN

Study of dynamical heterogeneities in colloidal nanoclay suspensions approaching dynamical arrest

Paramesh Gadige, Debasish Saha, Sanjay Kumar Behera & Ranjini Bandyopadhyay

The dynamics of aqueous Laponite clay suspensions slow down with increasing sample waiting time (t_w). This behavior, and the material fragility that results, closely resemble the dynamical slowdown in fragile supercooled liquids with decreasing temperature, and are typically ascribed to the increasing sizes of distinct dynamical heterogeneities in the sample. In this article, we characterize the dynamical heterogeneities in Laponite suspensions by invoking the three-point dynamic susceptibility formalism. The average time-dependent two-point intensity autocorrelation and its sensitivity to t_w are probed in dynamic light scattering experiments. Distributions of relaxation time scales, deduced from the Kohlrausch-Williams-Watts equation, are seen to widen with increasing t_w . The calculated three-point dynamic susceptibility of Laponite suspensions exhibits a peak, with the peak height increasing with evolving t_w at fixed volume fraction or with increasing volume fraction at fixed t_w , thereby signifying the slowdown of the sample dynamics. The number of dynamically correlated particles, calculated from the peak-height, is seen to initially increase rapidly with increasing t_w before eventually slowing down close to the non-ergodic transition point. This observation is in agreement with published reports on supercooled liquids and hard sphere colloidal suspensions and offers a unique insight into the colloidal glass transition of Laponite suspensions.

Glasses are characterized by amorphous order and solid-like rigidities and have a wide range of applications in our day-to-day lives^{1,2}. Supercooled liquids and slightly polydisperse colloidal suspensions form glasses as the relevant control parameters, temperature (T) and volume fraction (ϕ) respectively, are changed appropriately^{2,3}. Their dynamics slow down dramatically with decreasing T or with increasing ϕ and their viscosities (η) or structural relaxation timescales (τ_α) grow by several orders of magnitude. Below the glass transition temperature T_g or above the glass transition volume fraction ϕ_g ($\phi_g = 0.58$ for hard-sphere colloidal suspensions), η becomes so large that no flow or structural relaxation can be detected in the system. Glass-forming liquids are called strong if τ_α (or η) shows a nearly Arrhenius growth as a function of the relevant control parameter, whereas they are termed fragile if a super-Arrhenius trend is followed^{4,5}. In many theories and phenomenological models, the dynamical slowdown and the fragile behavior of glass-forming liquids are understood by considering the cooperative movement of the constituent molecules or particles of the glass-forming liquid^{6,7}. The distinct regions exhibiting correlated particle motion are called dynamical heterogeneities (DHs). The sizes of the DHs, or alternatively, the number of molecules or particles showing correlated movement (N_{corr}), grow as the glass transition is approached. The glass transition is manifested by a remarkable slowdown in the dynamics which results in the observed increase in τ_α . Simulations and experiments have established the presence of DHs⁸⁻¹⁰ and the growth of N_{corr} in glass-forming liquids through the calculation of multipoint correlation functions^{6,11-17}. Experimentally, such measurements in supercooled liquids are typically performed using non-linear dielectric susceptibility¹⁸⁻²¹.

The present work characterises the DHs in a fragile colloidal glass. Colloidal clay suspensions are known to exhibit rich phase behavior, showing fluid, gel, ordered and disordered phases²²⁻²⁵, and serve as excellent model systems to mimic the behaviour of atomic systems²⁶. One ubiquitous example of a model colloidal system is Laponite, a synthetic smectite clay which has been studied extensively for its soft glassy rheology²⁷ and interesting aging properties as it spontaneously transforms from a liquid to a glass with increasing time since sample preparation, the waiting time t_w ²⁸⁻³¹. In this article, we characterize the growth of N_{corr} in synthetic Laponite clay suspensions at several t_w . Aqueous suspensions of Laponite clay are known to form Wigner repulsive glasses^{23,29,32,33} in the concentration range 2–3.5 wt.% due to the buildup of long range inter-particle electrostatic repulsive

Soft Condensed Matter Group, Raman Research Institute, C. V. Raman Avenue, Sadashivanagar, Bangalore, 560 080, India. Correspondence and requests for materials should be addressed to R.B. (email: ranjini@rri.res.in)

interactions with increasing t_w ^{28,29}. The growth of the α -relaxation time in a super-Arrhenius manner as t_w increases has been established experimentally^{28,34,35} in Laponite suspensions. Recent studies in our group have established that the slowdown in the dynamics of Laponite suspensions resembles the slowdown reported in fragile glass-forming molecular liquids if t_w of the former system is mapped to $(1/T)$ of the latter in the Arrhenius and the Vogel-Fulcher-Tammann equations, which represent, respectively, the temperature dependences of the secondary and primary relaxation modes^{31,33,34,36}. In an earlier study, S. Jabbari-Farouji *et al.*^{37,38} reported DHs in Laponite suspensions by studying the particles' rotational and translational diffusion coefficients as a function of t_w . It was observed that the rotational diffusion of the constituent particles slows down at a faster rate than their translational motion. C. Maggi *et al.* showed collective motion and their growing sizes in aging Laponite suspensions using a time-resolved light scattering technique³⁹ which combines homodyne and heterodyne dynamic light scattering methods to extract the four-point susceptibility. In these experiments, the concentration of Laponite is 1.1 wt.% where Laponite is expected to form a gel²³.

In this study, we employ the three-point correlation function formalism^{15–17} to probe DHs and N_{corr} in Laponite suspensions of concentrations 3.0 wt.% and 3.25 wt.% with increasing t_w as well as by studying several concentrations between 2.0 to 3.5 wt.% (the corresponding volume fractions $\phi = 0.008$ to 0.014) at fixed t_w . For all Laponite suspensions studied here, a minute volume fraction of 100 nm diameter polystyrene beads are added as probe particles in dynamic light scattering experiments. For the concentration range of Laponite suspensions chosen in the present experiments, the suspensions are expected to form a repulsive glass²³. The relaxation dynamics of Laponite suspensions are studied by analysing the intensity autocorrelation functions obtained in homodyne dynamic light scattering experiments as a function of the waiting time of the Laponite suspension t_w at fixed ϕ and also by varying ϕ at fixed t_w . The scattering function decay curves are fitted by parametrizing the two-step relaxation equation (showing exponential and stretched exponential decays and representing, respectively, the secondary and primary relaxation processes of the Laponite suspension) with the control parameters t_w and ϕ . The three-point correlation functions, which are the t_w or ϕ derivatives of the decaying scattering function curves, are estimated in this analysis and are seen to exhibit peaks whose heights increase with increasing t_w or ϕ . N_{corr} is calculated from the peak height data and its evolution with $\langle \tau_{ww} \rangle / \tau_g$, where τ_g is the relaxation time at which the Laponite suspension enters the non-ergodic state, bears a striking resemblance to existing calculations for the growth of correlations in rapidly quenched supercooled liquids. We believe that our study, which demonstrates the existence of remarkable similarities between the kinetic arrest phenomena in Laponite clay suspensions and in supercooled liquids, provides valuable insight into the colloidal glass transition of Laponite suspensions.

Results and Discussion

Characterising the structural relaxation process. The intensity auto correlation function $g^{(2)}(q, t)$ in DLS⁴⁰ is related to the self-intermediate scattering function $F_s(q, t)$ by the Siegert relation^{41,42},

$$g^{(2)}(q, t) - 1 = A |F_s(q, t)|^2 \quad (1)$$

where

$$F_s(q, t) = \frac{1}{N} \left\langle \sum_j \exp\{iq \cdot [r_j(t) - r_j(0)]\} \right\rangle \quad (2)$$

Here, $r_j(t)$ is the position of particle j at time t , A is the spatial coherence factor and the brackets represent an ensemble average. $F_s(q, t)$ or the two-point correlation function quantifies the relaxation dynamics between delay times of 0 and t seconds. $F_s(q, t)$ vs. delay time plots are obtained using DLS experiments for aging Laponite clay suspensions at several waiting times t_w (Fig. 1(a)). Laponite particles are extremely weak scatterers of light. Since the motivation of this work is to calculate higher order correlation functions, we have ensured a high signal to noise ratio in our measurements by homogeneously dispersing a minute quantity of PS beads ($\phi_{PS} = 5.66 \times 10^{-5}$) in the Laponite suspensions. PS beads have a high dielectric constant mismatch with the solvent, thereby ensuring a strong scattered intensity signal⁴³. Furthermore, the low concentration of the PS beads ensures that $qR_{IPD} > 1$ (where R_{IPD} is the inter-particle distance and $q = 2.2 \times 10^{-2} \text{ nm}^{-1}$ for $\theta = 90^\circ$). PS particles are stabilized by negatively charged sulfate groups. The interactions between the PS and Laponite particles therefore remain repulsive. The addition of PS particles is not expected to affect the strong repulsive interactions that develop between the Laponite particles in the suspensions. The relaxation time of a 100 nm PS particle in water medium is 220 μs which is less than the characteristic structural relaxation time of 630 μs at $t_w = 0$ for a 2 wt% Lapo-PS suspension. The self-diffusion of the PS beads is therefore strongly affected by the aging of the underlying Laponite suspensions. Our experiments probe the collective behavior or heterogeneous dynamics of Lapo-PS particles in aqueous suspensions. The acquired data in Fig. 1(a) corresponds to the self-intermediate scattering function of the PS particles mixed uniformly in the clay suspension. The normalized $F_s(q, t)$ plots in Fig. 1(a) are seen to decay comparatively faster for smaller t_w values. As t_w increases, the decay of $F_s(q, t)$ slows down considerably. Furthermore, the decay of $F_s(q, t)$ can be described as a two-step process³⁴ comprising a fast decaying exponential part and a comparatively slower stretched exponential part^{31,35,36,44} and can be expressed as

$$F_s(q, t) = a \exp\{-t/\tau_1\} + (1 - a) \exp\{-(t/\tau_{ww})^\beta\} \quad (3)$$

Here, τ_1 is the fast or secondary relaxation time (corresponding to the diffusion of a Laponite particle inside the cage formed by the neighbors), τ_{ww} is the structural or primary α -relaxation time (representing its cooperative diffusion to a neighbouring position), β is a stretching exponent, and a is the weight factor for the faster secondary relaxation process³⁴. Fits of the experimental data to Eq. 3 are shown in Fig. 1(a) for $C_L = 3.0$ wt.% and the fitting

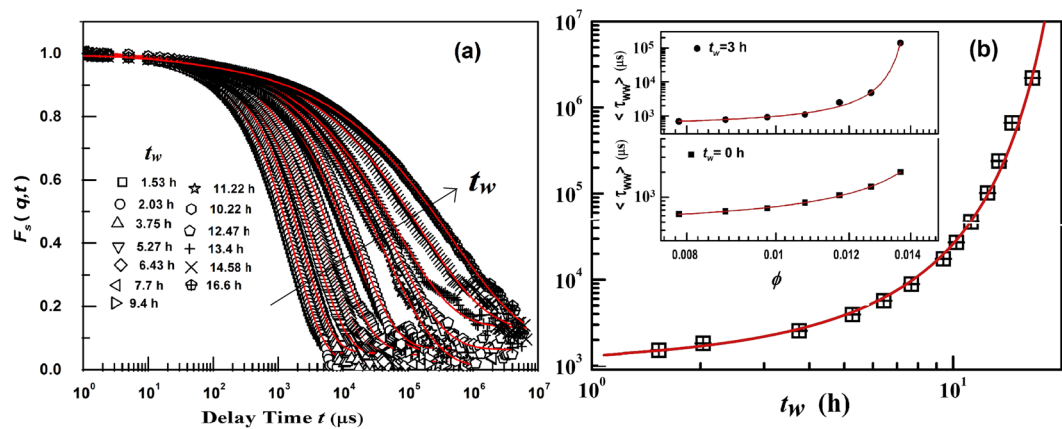


Figure 1. (a) Self intermediate intensity scattering functions ($F_s(q, t)$ decay curves) vs. delay times recorded at various waiting times (t_w) at $\theta = 90^\circ$ ($q = 2.2 \times 10^{-2} \text{ nm}^{-1}$). Solid lines are fits to the two step relaxation function given in Eq. 3 and the fitting parameters obtained with increasing t_w are given in the Supporting Information, Table S1. (b) Mean structural relaxation time ($\langle \tau_{ww} \rangle$) as a function of t_w for a Laponite-PS suspension of concentration $C_L = 3.0$ wt.%, and PS volume fraction $\phi_{PS} = 5.66 \times 10^{-5}$. The solid line is a fit to Eq. 4. The inset in Fig. 1(b) shows the plots of $\langle \tau_{ww} \rangle$ vs. ϕ at fixed $t_w = 0$ h (bottom) and 3 h (top). Solid lines are fits to the VFT (Eq. 5) with ϕ as control parameter.

parameters a , τ_{ww} and β , obtained from the fits for several t_w , are shown in Table S1 in Supporting Information (SI). $F_s(q, t)$ is also recorded as a function of Laponite concentration $C_L = 2.0$ wt.% to 3.5 wt.%, i.e. changing ϕ . In these experiments, the dynamics are probed at fixed t_w values 0 h and 3 h. The corresponding $F_s(q, t)$ vs. delay time curves along with fits to Eq. 3 with changing ϕ are given in SI (Fig. S1) at $t_w = 0$ and 3 h. Fitting parameters are listed in Table S2 ($t_w = 0$ h) and Table S3 ($t_w = 3$ h) with varying ϕ . We find good fits when τ_1 , corresponding to the diffusion of a single Laponite particle, is kept fixed at $30 \mu\text{s}$ ³⁴. It was reported for glassy Laponite suspensions that the fast relaxation time τ_1 ($= 30 \mu\text{s}$) is close to the diffusive motion of individual Laponite particles according to the Stokes-Einstein relation³⁴. The dynamics probed by PS particles in clay suspensions can therefore be attributed to Laponite particle dynamics. This feature is discussed in detail in Supporting Information and ensures that the PS particles do not, in any way, interfere with the cage formation dynamics of the Laponite particles and the structural relaxation process. The growth in the structural relaxation time τ_{ww} arises from an evolution of the screened interparticle electrostatic repulsion due to a gradual process of tactoid exfoliation⁴⁵. The dependence of the mean structural relaxation time $\langle \tau_{ww} \rangle = (\tau_{ww}/\beta)(\Gamma(1/\beta))$ ⁴⁶ on t_w is obtained from the fits and is plotted in Fig. 1(b). The ϕ dependence of $\langle \tau_{ww} \rangle$ at fixed $t_w = 0$ and 3 h are depicted in the insets of Fig. 1(b). Fragility^{4,5} of the colloidal glasses is studied by the modified Vogel-Fulcher-Tammann (VFT) equation in which $1/T$ is replaced by ϕ (the relevant control parameter for colloidal glasses)⁴⁷. Since Laponite suspensions transform to a non-ergodic state as t_w increases, therefore t_w has been used as the control parameter to study the Laponite glassy dynamics^{31, 33–36, 44, 48}. The fragile behavior of Laponite suspensions is studied by employing the modified VFT equation in which ϕ is replaced by t_w ^{34, 36} such that the modified VFT equation can be written as follows^{33, 34, 36}:

$$\langle \tau_{ww} \rangle = \tau_0 \exp\left(\frac{Dt_w}{t_\infty - t_w}\right) \quad (4)$$

In this equation, $\tau_0 = \tau_\alpha(t_w \rightarrow 0)$, D is the fragility parameter (the inverse of D quantifies the apparent deviation from the Arrhenius trend), and t_∞ is the waiting time at which the relaxation time diverges. The above equation is fitted to the data shown in Fig. 1(b) with fitting parameters, $\tau_0 = 1060 \pm 65 \mu\text{s}$, $D = 6.8 \pm 0.5$ and $t_\infty = 31.3 \pm 1.3$ h. Such a VFT like growth of $\langle \tau_{ww} \rangle$ with increasing t_w as the Laponite suspension approaches eventual kinetic arrest is strongly reminiscent of the observations reported in fragile molecular supercooled liquids with decreasing temperature T and in many hard sphere colloidal glasses with increasing volume fraction ϕ ¹⁷. The VFT equation where ϕ is the control parameter is given below

$$\langle \tau_{ww} \rangle = \tau_0 \exp\left(\frac{D\phi}{\phi_\infty - \phi}\right) \quad (5)$$

where $\tau_0 = \tau_\alpha(\phi \rightarrow 0)$ and ϕ_∞ is the volume fraction at which the relaxation time diverges. The plots of $\langle \tau_{ww} \rangle$ vs. ϕ , along with fits to Eq. 5, are shown in the insets of Fig. 1(b) at $t_w = 0$ h and 3 h. The fitting parameter are $\tau_0 = 395 \pm 22 \mu\text{s}$, $D = 0.57 \pm 0.02$, $\phi_\infty = 0.01852 \pm 0.0002$ at $t_w = 0$ and $\tau_0 = 471 \pm 50 \mu\text{s}$, $D = 0.33 \pm 0.02$ at $t_w = 3$ h, $\phi_\infty = 0.01442 \pm 0.0002$. It is seen that ϕ_∞ decreases with increasing t_w . Low concentration Laponite suspensions are expected to take a longer time to reach the arrested state i.e they will have large t_∞ . In this work, aging dynamics are probed in detail at two different concentrations, $C_L = 3.0$ and 3.25 wt.%. The $F_s(q, t)$ decay curves and fits to Eq. 3 for $C_L = 3.25$ wt.% are shown in SI (Fig. S2(a)). The fitting parameters for a fit to Eq. 4 are $\tau_0 = 1212 \pm 30 \mu\text{s}$, $D = 8.02 \pm 0.2$ and $t_\infty = 30.0 \pm 0.5$ h for $C_L = 3.25$ wt.%. The data is shown in Fig. S2(b).

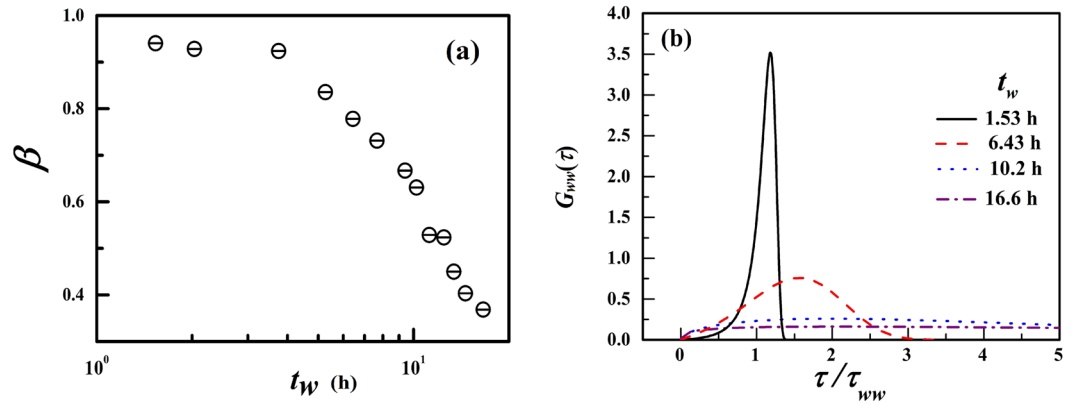


Figure 2. (a) The stretching exponent β vs. t_w and (b) the distribution of relaxation time scales $G_{ww}(\tau)$ plotted at various t_w for the Laponite-PS system $C_L = 3.0$ wt.% of Fig. 1.

Typically, the fragile behavior of glass-forming liquids as they approach the glass transition is rationalized by enumerating the number of particles engaged in slow correlated motion, N_{corr} in the DHs and the growing sizes of these regions of cooperative motion. The β values, obtained from Eq. 3, are plotted as a function of t_w and shown in Fig. 2(a). The decrease in β implies that the width of time scale distributions characterising the dynamics of independently relaxing DHs increases monotonically with increasing t_w . The correlated dynamics can therefore be modelled by assuming a linear superposition of exponential relaxation processes of the DHs, with each DH having its own relaxation time τ ¹⁵. The distribution functions of the relaxation times ($G_{ww}(\tau)$) with increasing t_w of the Laponite suspensions are calculated using the following Kohlrausch-Williams-Watts equation⁴⁶

$$\rho_{ww}(\tau) = -\frac{\tau_{ww}}{\pi\tau^2} \sum_{k=0}^{\infty} \frac{(-1)^k}{k!} \sin(\pi\beta k) \Gamma(\beta k + 1) \left(\frac{\tau}{\tau_{ww}}\right)^{(\beta k + 1)} \quad (6)$$

The distribution $G_{ww}(\tau) = \tau \rho_{ww}(\tau)$ at $t_w = 1.53, 6.43, 10.2$ and 16.6 h are plotted in Fig. 2(b) for $C_L = 3.0$ wt.%. A Laponite suspension lying in the liquid-like regime (*i.e.* at small t_w values) is characterised by a G_{ww} which shows a sharp peak at τ/τ_{ww} close to 1. In contrast, as the sample ages towards a non-ergodic state, a broad distribution of G_{ww} having peak position at $\tau/\tau_{ww} > 1$ is observed. This suggests that at small sample ages, the relaxation timescales characterising the reorganization dynamics is more likely to have values within a narrow range. The broad distribution at longer t_w can be rationalized by considering the presence of simultaneous fast and slow moving cooperatively rearranging regions having their own independent relaxation times. The broadening of G_{ww} with increase in the control parameter t_w is reminiscent of observations in fragile supercooled liquids with decreasing T ^{12, 14} and strongly indicates the presence of heterogeneous dynamics in aging colloidal Laponite suspensions.

Characterizing dynamical heterogeneities by evaluating three-point correlation functions. Characterizing N_{corr} of DHs in experiments is a challenging task. Theoretically, information about the sizes of the DHs and N_{corr} are embedded in the four point dynamic susceptibility which takes into account correlations in both space and time. A detailed theoretical and mathematical treatment of the four point correlation function and its relation to N_{corr} can be found in the literature^{49, 50}. The four-point dynamic susceptibility $\chi_4(q, t)$ is related to the fluctuating part of the self-intermediate scattering function $\delta F_s(q, t)$ by the following equation:

$$\chi_4(q, t) = N_{corr} \langle \delta F_s(q, t)^2 \rangle \quad (7)$$

Experimentally therefore, χ_4 can be obtained by resolving the dynamical behavior of the observable in both space and time. In contrast to molecular systems, colloidal particles have comparatively larger sizes ($10\text{ nm} - 1\ \mu\text{m}$). This feature, and the easy tunability of inter-particle interactions, make colloidal systems robust model candidates for experimental and simulation studies of a variety of physical phenomena. Indeed, χ_4 has been extracted for colloidal glasses using advanced microscopy techniques and simulations^{6, 13, 51}. Maggi *et al.*³⁹ established the growth of the four-point dynamic susceptibility (extracted from a combined homodyne and heterodyne DLS technique) as aging progresses in a low concentration (1.1 wt.%) Laponite suspension which is known to form a gel over a long time²³. Since computation of spatial correlations from experimental data for molecular and nanocolloidal suspensions, *eg.* Laponite, is difficult, therefore in order to study DHs, a three-point correlation function, which is the lower bound of the four-point correlation function, has been introduced^{18, 52, 53}. It can be accessed experimentally by probing the sensitivity of the two-point correlation function (dielectric response or the scattering function) to external control parameters such as T in supercooled liquids and ϕ in colloidal systems. For hard sphere colloids, $\chi_4(q, t)$ is written as^{17, 18}

$$\chi_4(q, t) = \chi_4(q, t)|_{\phi} + \rho k_B T k_T [\phi \chi_{\phi}(q, t)]^2 \quad (8)$$

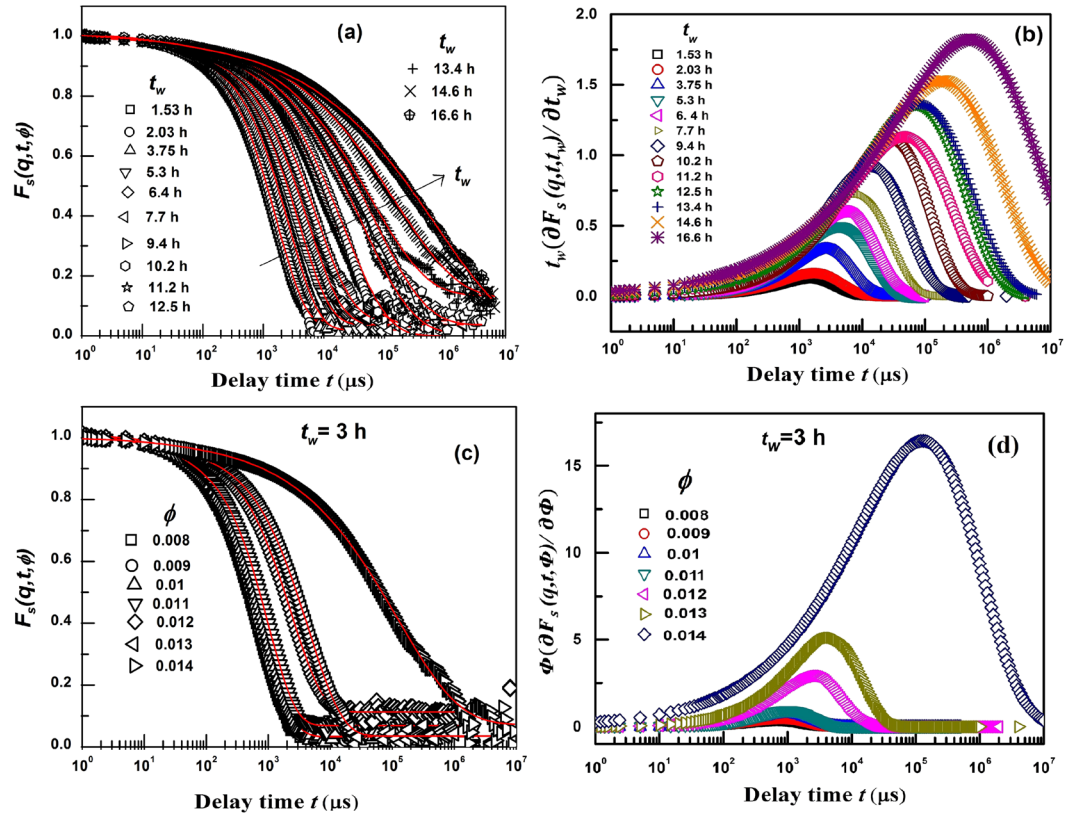


Figure 3. (a) $F_s(q, t, t_w)$ decay curves at various t_w for Laponite-PS suspensions (Laponite concentration $C_L = 3.0$ wt.%, and PS volume fraction $\phi_{PS} = 5.66 \times 10^{-5}$). The solid lines are fits to Eq. 9. (b) Plots of $\chi_{t_w}(q, t) = t_w \partial F_s(q, t, t_w) / \partial t_w$ as a function of delay time t for curves shown in Fig. 3(a). (c) $F_s(q, t, \phi)$ decay curves at various ϕ at $t_w = 3$ h. The solid lines are fits to Eq. 10. (d) Plots of $\chi_\phi(q, t) = \phi \partial F_s(q, t, \phi) / \partial \phi$ as a function of delay time t for curves shown in Fig. 3(c).

where $\chi_4(q, t)|_\phi$ is the fixed density value of $\chi_4(q, t)$, ρ is the particle number density, k_T is the isothermal compressibility and $\chi_\phi(q, t)$ is the derivative of $F_s(\tau_\alpha, \beta)$ with respect to ϕ . The second term in Eq. 8 is the three-point dynamic susceptibility and can be accessed experimentally. The derivative of $F_s(\tau_\alpha, \beta)$ with respect to ϕ , $\chi_\phi(q, t)$, has been obtained in dynamic light scattering experiments for colloidal systems¹⁷, while in supercooled liquids, the thermal derivative of the dielectric response χ_T has been used to study N_{corr} ¹⁵. In these experiments, $\chi_\phi(q, t)$ and χ_T were evaluated by probing, respectively, the scattering function and dielectric response at infinitesimal regular intervals of ϕ and T . The ϕ -dependence of $F_s(q, t)$ or the T dependence of the dielectric spectrum were fitted with polynomial functions. The derivatives of these fitted curves with respect to the control parameter yield the three-point susceptibilities. The use of the three point correlation function formalism to calculate N_{corr} in a wide range of glass forming liquids using dielectric and light scattering data has been successfully demonstrated by Dalle-Ferrier *et al.*^{15,16}. The authors showed that $\chi_\phi(q, t)$ and χ_T show peaks similar to χ_4 , with the peak heights proportional to N_{corr} .

In the present study, the procedure outlined above is implemented to obtain N_{corr} for aging Laponite colloidal suspensions at concentrations where they are expected to form a repulsive glass. In this regime, t_w is expected to behave as the control parameter for slowdown of the dynamics and is analogous to ϕ for hard sphere colloids^{34,35,44}. We also compare the results of Laponite dynamics with increasing ϕ , the usual control parameter for colloidal glasses at fixed t_w . Our studies involve the computation of the sensitivity of $F_s(q, t)$ with respect to changes in t_w and ϕ to extract the three-point correlation functions. The dependence of $F_s(q, t)$ on t_w is shown in Fig. 3(a) for $C_L = 3.0$ wt.% and in Fig. 3(c) while varying ϕ at $t_w = 3$ h. The derivatives of $F_s(q, t)$ with respect to t_w and ϕ are obtained by parametrizing Eq. 3 with Eq. 4 to study aging by varying t_w . Furthermore to analyse the data at several ϕ at fixed $t_w = 0$ and 3 h, Eq. 3 is parametrized with Eq. 5. The equations are given by

$$F_s(q, t, t_w) = a \exp\{-t/\tau_1\} + (1 - a) \exp\left\{-\left[t/\left\{\tau_0 \exp\left(\frac{Dt_w}{t_\infty - t_w}\right)\right\}\right]^\beta\right\} \quad (9)$$

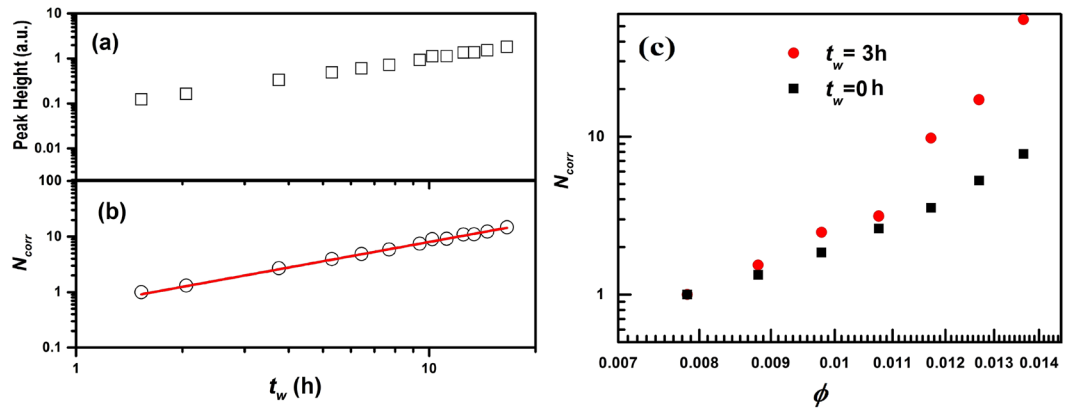


Figure 4. (a) Growth of peak height and (b) N_{corr} calculated from the data in Fig. 3(b) vs. t_w as the sample approaches the non-ergodic state. The solid line in (b) is a power law fit of the form $N_{corr} = B(t_w)^\gamma$ where $\gamma = 1.17 \pm 0.02$ and $B = 0.56 \pm 0.04$. (c) N_{corr} vs. ϕ at $t_w = 0$ and 3 h.

$$F_s(q, t, \phi) = a \exp\{-t/\tau\} + (1 - a) \exp\left\{-\left[t/\tau_0 \exp\left(\frac{D\phi}{\phi_\infty - \phi}\right)\right]\right\}^\beta \quad (10)$$

The $F_s(q, t, t_w)$ decay curves, fitted to Eqs 9 and 10, are depicted in Fig. 3(a) using solid lines for $C_L = 3.0$ wt.% and in Fig. 3(c) with varying ϕ at $t_w = 3$ h, (for $t_w = 0$ h, plots are shown in Fig. S3 of SI), respectively. The fitting parameters thus obtained are in good agreement with the parameters extracted by fitting the data to Eq. 3 and are tabulated in Tables S5 and S6 of the SI. The three-point correlation functions for Laponite suspensions, $\chi_{t_w}(q, t)$ and $\chi_\phi(q, t)$, are obtained by differentiating the fitted curves shown in Fig. 3(a) with respect to t_w , i.e. $\chi_{t_w}(q, t) = t_w \frac{\partial F_s(q, t, t_w)}{\partial t_w}$ and for Fig. 3(c) with respect to ϕ i.e. $\chi_\phi(q, t) = \phi \frac{\partial F_s(q, t, \phi)}{\partial \phi}$. The calculated derivatives, shown in Fig. 3(b) and (d) with increasing t_w at fixed ϕ and with increasing ϕ at fixed t_w , respectively, exhibit peaks, with the peak heights increasing and the peak positions shifting to higher delay times t with increasing value of the control parameters. Plots of fits to Eq. 9 and $\chi_{t_w}(q, t)$ curves for $C_L = 3.25$ wt.% are given in Fig. S3 of SI. ($\chi_\phi(q, t)$ at $t_w = 0$ h curves are shown in Fig. S4).

It has been shown that the peak heights of the three-point susceptibility in molecular liquids (control parameter T) and hard sphere colloids (control parameter ϕ) contain information of N_{corr} . The peak heights of three point susceptibilities deduced in the present case with t_w as control parameter at fixed ϕ and with ϕ as control parameter at fixed t_w can therefore be expected to contain information on N_{corr} for the aging Laponite suspensions studied here. The observed growth of the peak height of $\chi_{t_w}(q, t)$ and $\chi_\phi(q, t)$, with increasing t_w or increasing ϕ establish the growing dynamical heterogeneities and the monotonically increasing trend of N_{corr} during the spontaneous aging process of Laponite colloidal suspensions. The height of the peaks, plotted in Fig. 4(a) (for $C_L = 3.0$ wt.%) as a function of t_w , is proportional to N_{corr} ¹⁵. Next, $N_{corr} \propto \left[t_w \left(\frac{\partial F_s(q, t, t_w)}{\partial t_w}\right)\right]$ or $N_{corr} \propto \left[\phi \left(\frac{\partial F_s(q, t, \phi)}{\partial \phi}\right)\right]$ are calculated with the assumption that for the smallest waiting times or lowest ϕ , correlated particle motion can be ruled out (with particles moving independently, i.e. $N_{corr} = 1$). Here, normalization is carried out with the peak height at $t_w = 1.5$ h for t_w dependent study of $C_L = 3.0$ wt % or with $\phi = 0.008$ ($C_L = 2.0$ wt %) for ϕ dependent data to obtain N_{corr} . Since at $t_w = 1.5$ h and $\phi = 0.008$, the stretching exponent, β is close to one and the distribution function of relaxation times G_{ww} peaks close to $\tau/\tau_{ww} = 1$ as shown in Fig. 2 (for $t_w = 1.5$ h, $\beta = 0.94 \pm 0.01$ and $\tau/\tau_{ww} = 1.18$, just starting to deviate from unity). τ/τ_{ww} close to one suggests the presence of a unique relaxation time and the absence of correlated motion of the particles in suspension. The proportionality pre-factors in the relation for N_{corr} can be assumed to be independent of t_w at fixed ϕ as number density of Laponite particles is constant. It is to be noted here that there exists initial osmotic swelling of Laponite particles during preparation of suspensions due to hydration which is followed by build up of electrostatic repulsive interactions between the particles²³. Therefore, over the range of aging times probed in the present experiments, the osmotic pressure and the values of k_T is expected to be constant. Finally, $\left[t_w \left(\frac{\partial F_s(q, t, t_w)}{\partial t_w}\right)\right]$ is normalized with respect to the value at $t_w = 1.5$ h at all t_w to obtain N_{corr} as a function of t_w for $C_L = 3.0$ wt.%. The corresponding N_{corr} plot is given in Fig. 4(b). N_{corr} obtained with increasing ϕ is shown in Fig. 4(c) at $t_w = 0$ and 3 h. We observe a small increase in N_{corr} at $t_w = 0$ h with increasing ϕ and obtain a large N_{corr} at high ϕ at higher t_w ($= 3$ h). This is because samples of higher concentration reach the non-ergodic state at lower t_w . Growth of peak height and N_{corr} for $C_L = 3.25$ wt.% are plotted in SI (Fig. S5) and similar trends were observed as $C_L = 3.0$ wt. %. If $\tau_g = 10$ s is defined as the non-ergodic transition point¹⁵, a monotonic growth of N_{corr} with increasing t_w is observed. The growth of N_{corr} shows a power law dependence on t_w ($N_{corr} = B(t_w)^\gamma$), where the exponent $\gamma = 1.17 \pm 0.02$, $B = 0.56 \pm 0.04$) and is shown by a solid line in Fig. 4(b) for $C_L = 3.0$ wt.%. Similar power law growth of N_{corr} is observed for measurements (upto $t_w = 9.6$ h) performed at a lower scattering angle $\theta = 75^\circ$ ($q = 1.9 \times 10^{-2} \text{ nm}^{-1}$) and 60°

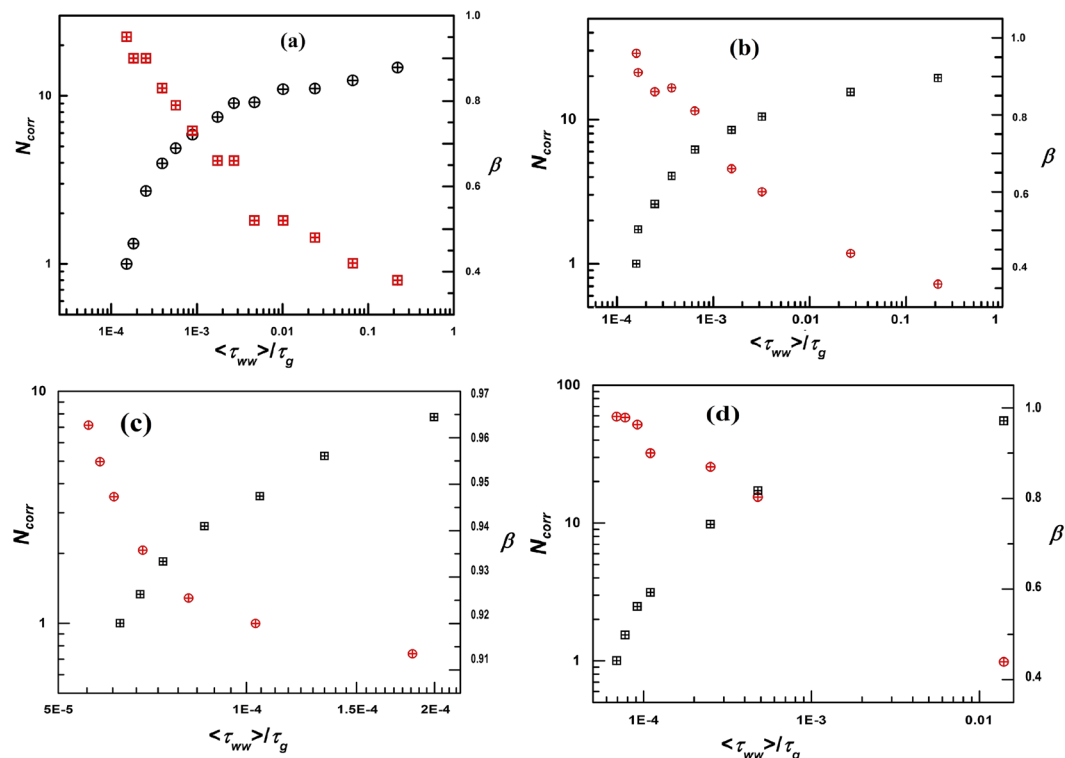


Figure 5. (a) Plot of N_{corr} (black symbols) and β (red symbols) vs. $\langle \tau_{ww} \rangle / \tau_g$ for $C_L = 3.0$ wt.%, (b) for $C_L = 3.25$ wt.%. (c) with increasing ϕ at $t_w = 0$ h and (d) with increasing ϕ at $t_w = 3$ h. N_{corr} shows a monotonic increase, with the initial rapid increase slowing down considerably at high $\langle \tau_{ww} \rangle / \tau_g$ while β shows a monotonic decrease.

($q = 1.57 \times 10^{-2} \text{ nm}^{-1}$) (thereby probing longer length scales $1/q$ and is displayed in the SI in Fig. S6 for $C_L = 3.0$ wt.%. Slightly higher N_{corr} values are observed at lower q due to the large probed length scales (45 nm to 63.6 nm for studied q values).

In Fig. 5, N_{corr} is plotted as a function of τ_{ww} normalized with $\tau_g = 10 \text{ s}^{15}$ to observe its evolution for $C_L = 3.0$ wt.% (Fig. 5(a)), 3.25 wt.% (Fig. 5(b)) and with increasing ϕ at $t_w = 0$ and 3 h (Fig. 5(c) and (d) respectively). β values are also plotted in all the figures in order to correlate the evolution of the time scale distributions with growth of N_{corr} . The decrease of β (or increase in the width of distribution of relaxation time scales, G_{ww} , as shown in Fig. 2(b)) as Laponite suspensions approach non-ergodicity indicates that the dynamics turn progressively heterogeneous. This implies growing correlations in the system, *i.e.* the appearance of a large number of regions of correlated groups of particles with distinct average relaxation times as the waiting time of the suspension increases. The appearance of dynamical heterogeneities of larger sizes (characterised by larger N_{corr}) results in a slowdown of the dynamics which manifests as a fragile supercooled liquid-like growth of $\langle \tau_{ww} \rangle$ (VFT-like plot in Fig. 1(b)). However, it is seen that N_{corr} grows rapidly at small $\langle \tau_{ww} \rangle / \tau_g$, but slows down considerably as the suspensions approach the non-ergodic transition point. Remarkably, this trend is in close agreement with an observation in supercooled liquids in which N_{corr} is reported to show a power-law dependence at large T (*i.e.* in the liquid regime) and a logarithmic growth at low T (*i.e.* near the glass transition)^{15,16}. The slow increase of N_{corr} close to the non-ergodic transition is attributed to activated dynamics. In this regime, cooperative motion becomes increasingly difficult as the structural rearrangement time slows down dramatically as a consequence of the very high viscosity of the system and results in large $\langle \tau_{ww} \rangle$ values. Activated dynamics close to the glass transition is also seen in hard sphere glasses¹⁷. The increasing values of N_{corr} with t_w , estimated from the three-point dynamic susceptibility in the present study therefore provides a quantitative measure of the fragile supercooled liquid-like heterogeneous dynamics in soft glassy colloidal Laponite suspensions.

Conclusions

Dynamical heterogeneities in aging Laponite colloidal suspensions are investigated by the three-point dynamic susceptibility formalism with respect to the control parameters, t_w and ϕ . Laponite colloidal suspensions exhibit fragile supercooled liquid-like dynamics, with the average structural relaxation time, $\langle \tau_{ww} \rangle$, in its characteristic two-step relaxation process exhibiting a VFT-like growth as a function of t_w at fixed ϕ and with varying ϕ at fixed t_w . The three-point dynamic susceptibility is computed from DLS experiments by taking the derivatives of the two-point scattering decay function, $F_s(q, t)$, with respect to t_w and ϕ . The three-point dynamic susceptibility exhibits a peak, with the peak height growing with increasing t_w or ϕ . Our calculations show that N_{corr} , the number of particles participating in correlated motion, thereby setting the size of the dynamical heterogeneity, shows a power law increase with increase in the aging time t_w of the Laponite suspension. Furthermore, we show that the growth

of N_{corr} is initially quite fast, before slowing down close to the nonergodic transition. We believe that our study provides valuable insight into the approach of repulsive glass-forming Laponite suspensions towards kinetic arrest by demonstrating that the growth of correlations in these suspensions closely resemble the observations reported for fragile supercooled liquids¹⁵. Unlike in fragile supercooled liquids, however, the dynamics of Laponite suspensions are driven by athermal processes such as long-range screened inter-particle electrostatic repulsions and tactoid exfoliation. Given the similarities in the dynamical slowdown processes and the growth of correlations in Laponite suspensions and fragile supercooled liquids, the ubiquitous kinetic slowdown in glass-forming liquids, driven by a growth in heterogeneous dynamics, could well be a universal feature of fragile glass-formers.

Sample preparation and experimental methods. Laponite RD[®] (BYK, Inc.) powder was procured from Southern Clay products. As clay particles are hygroscopic in nature, the powder was dried in a hot oven at 120 °C for 16 h. $C_L = 2, 2.25, 2.5, 2.75, 3.0, 3.25$ and 3.5 wt % Laponite concentration ($\phi_L = 1.18 \times 10^{-2}$) suspensions were prepared by adding the dried powder slowly to Milli-Q water (resistivity 18.2 M Ω -cm). C_L was chosen to lie in a region of the phase space where the Laponite suspension is expected to form a Wigner glass^{23,32}. The suspension was stirred vigorously for 1 h using a magnetic stirrer. The resulting optically clear and homogeneous suspension was filtered using a 0.45 μ m Millipore Millex-HV grade filter using a syringe pump at a constant flow rate of 3 ml/min. A very small volume fraction ($\phi_{PS} = 5.66 \times 10^{-5}$) of polystyrene (PS) probe particles (100 nm in diameter) was added and mixed homogeneously. The PS particles having polydispersity of 5 to 10% and stabilized with negatively charged sulfate groups are obtained from Bangs Lab (USA). These PS beads (whose sizes are less than the wavelength of the light used) are expected to act as light scatterers in the otherwise highly transparent Laponite suspensions⁴³. The Laponite-PS suspensions were subsequently sealed in a cuvette. The waiting time, t_w , was calculated from the time when the stirring of the suspension was stopped and the cuvette was sealed. Auto-correlation functions of the intensity scattered by these suspensions were recorded in dynamic light scattering (DLS) experiments⁴⁰ using a Brookhaven Instruments Corporation BI-200SM spectrometer and a BI-9000AT digital autocorrelator. A constant temperature of 25 °C was maintained using a temperature controller (Polyscience Digital) attached to the DLS system. Details of the set-up are given elsewhere³⁴. The normalized intensity autocorrelation function of the scattered light, $g^{(2)}(q, t) = \frac{\langle I(q,0)I(q,t) \rangle}{\langle I(q,0) \rangle^2}$, was recorded as a function of delay time t . Here, q and $I(q, t)$ are the scattering wave vector and the intensity of the scattered light at a particular q and t respectively. q is related to the scattering angle θ by the equation $q = (4\pi n/\lambda)\sin(\theta/2)$, where n and λ are the refractive index of the medium ($n = 1.334$) and the wavelength of the laser ($\lambda = 532$ nm) respectively⁴⁰. The intensity autocorrelation data was recorded at $\theta = 90^\circ$ ($q = 2.2 \times 10^{-2}$ nm⁻¹), $\theta = 75^\circ$ ($q = 1.9 \times 10^{-2}$ nm⁻¹) and $\theta = 60^\circ$ ($q = 1.6 \times 10^{-2}$ nm⁻¹). The three point correlation functions were computed by taking the derivatives of the time-dependent self-intermediate scattering function using Mathematica with respect to t_w at fixed $C_L = 3.0$ and 3.25 wt. % and with respect to ϕ at fixed $t_w = 0$ and 3 h for all the concentrations studied.

References

1. Wolynes, P. G. & Lubchenko, V. *Structural Glasses and Supercooled Liquids: Theory, Experiment, and Applications*, John Wiley & Sons, New Jersey (2012).
2. Ediger, M. D., Angell, C. A. & Nagel, S. R. Supercooled Liquids and Glasses. *J. Phys. Chem.* **100**, 13200–13212 (1996).
3. Pusey, P. N. & van Megen, W. Phase behaviour of concentrated suspensions of nearly hard colloidal spheres. *Nature (London)* **320**, 340 (1986).
4. Angell, C. A. Formation of Glasses from Liquids and Biopolymers. *Science* **267**, 1924 (1995).
5. Angell, C. A. Relaxation in liquids, polymers and plastic crystals $\alpha\beta$ strong/fragile patterns and problems. *J. Non-Cryst. Solids* **131–133**, 13–31 (1991).
6. *Dynamical Heterogeneities in Glasses, Colloids and Granular Media*, edited by Berthier, L., Biroli, G., Bouchaud, J.-P., Cipelletti, L. & van Saarloos, W. Oxford University Press, New York (2010).
7. Adam, G. & Gibbs, J. H. On the Temperature Dependence of Cooperative Relaxation Properties in Glass — Forming Liquids. *J. Chem. Phys.* **43**, 139 (1965).
8. Richert, R. Heterogeneous dynamics in liquids: fluctuations in space and time. *J. Phys.: Condens. Matter* **14**, R703 (2002).
9. van de Laar, T., Higler, R., Schroën, K. & Sprakel, J. Discontinuous nature of the repulsive-to-attractive colloidal glass transition. *Sci. Rep.* **6**, 22725 (2016).
10. Haddadian, E. J. *et al.* Comparative Study of the Collective Dynamics of Proteins and Inorganic Nanoparticles. *Sci. Rep.* **7**, 41671 (2017).
11. Stevenson, J. D., Schmalian, J. & Wolynes, P. G. The shapes of cooperatively rearranging regions in glass-forming liquids. *Nature Phys.* **2**, 268 (2006).
12. Ediger, M. D. Spatially heterogeneous dynamics in supercooled liquids. *Annu. Rev. Phys. Chem.* **51**, 99 (2000).
13. Zhang, Z., Yunker, P. J., Habdas, P. & Yodh, A. G. Cooperative Rearrangement Regions and Dynamical Heterogeneities in Colloidal Glasses with Attractive Versus Repulsive Interactions. *Phys. Rev. Lett.* **107**, 208303 (2011).
14. Debenedetti, P. G. & Stillinger, F. H. Supercooled liquids and the glass transition. *Nature (London)* **410**, 259 (2001).
15. Dalle-Ferrier, C. *et al.* Spatial correlations in the dynamics of glassforming liquids: Experimental determination of their temperature dependence. *Phys. Rev. E* **76**, 041510 (2007).
16. Dalle-Ferrier, C., Eibl, S., Pappas, C. & Alba-Simionesco, C. Temperature dependence of three-point correlation functions of viscous liquids: the case of glycerol. *J. Phys.: Condens. Matter* **20**, 494240 (2008).
17. Brambilla, G., El Masri, D., Pierno, M., Berthier, L. & Cipelletti, L. Probing the Equilibrium Dynamics of Colloidal Hard Spheres above the Mode-Coupling Glass Transition. *Phys. Rev. Lett.* **102**, 085703 (2009).
18. Berthier, L. *et al.* Direct experimental evidence of a growing length scale accompanying the glass transition. *Science* **310**, 1797 (2005).
19. Crauste-Thibierge, C. *et al.* Evidence of Growing Spatial Correlations at the Glass Transition from Nonlinear Response Experiments. *Phys. Rev. Lett.* **104**, 165703 (2010).
20. Brun, C. *et al.* Nonlinear dielectric susceptibilities: Accurate determination of the growing correlation volume in a supercooled liquid. *Phys. Rev. B* **84**, 104204 (2011).
21. Bauer, T., Lunkenheimer, P. & Loidl, A. Cooperativity and the Freezing of Molecular Motion at the Glass Transition. *Phys. Rev. Lett.* **111**, 225702 (2013).
22. Cummins, H. Z. Liquid, glass, gel: The phases of colloidal Laponite. *J. Non-Cryst. Solids* **353**, 3891 (2007).

23. Ruzicka, B. & Zaccarelli, E. A fresh look at the Laponite phase diagram. *Soft Matter* **7**, 1268 (2011).
24. Shahin, A. & Joshi, Y. M. Irreversible Aging Dynamics and Generic Phase Behavior of Aqueous Suspensions of Laponite. *Langmuir* **26**, 4219 (2010).
25. Angelini, R. *et al.* Glass–glass transition during aging of a colloidal clay. *Nat. Commun.* **5**, 4049 (2014).
26. Manoharan, V. N. Colloidal matter: Packing, geometry, and entropy. *Science* **349**, 1253751 (2015).
27. Sollich, P., Lequeux, F., Hèbraud, P. & Cates, M. E. Rheology of Soft Glassy Materials. *Phys. Rev. Lett.* **78**, 2020 (1997).
28. Mourchid, A., Lecolier, E., Van Damme, H. & Levitz, P. On Viscoelastic, Birefringent, and Swelling Properties of Laponite Clay Suspensions: Revisited Phase Diagram. *Langmuir* **14**, 4718 (1998).
29. Bandyopadhyay, R. *et al.* Evolution of Particle-Scale Dynamics in an Aging Clay Suspension. *Phys. Rev. Lett.* **93**, 228302 (2004).
30. Joshi, Y. M. Model for cage formation in colloidal suspension of laponite. *J. Chem. Phys.* **127**, 081102 (2007).
31. Saha, D., Joshi, Y. M. & Bandyopadhyay, R. Characteristics of the secondary relaxation process in soft colloidal suspensions. *Europhys. Lett.* **112**, 46004 (2015).
32. Bonn, D., Tanaka, H., Wegdam, G., Kellay, H. & Meunier, J. Aging of a colloidal “Wigner” glass. *Europhys. Lett.* **45**, 52–57 (1998).
33. Saha, D., Bandyopadhyay, R. & Joshi, Y. M. Dynamic Light Scattering Study and DLVO Analysis of Physicochemical Interactions in Colloidal Suspensions of Charged Disks. *Langmuir* **31**, 3012 (2015).
34. Saha, D., Joshi, Y. M. & Bandyopadhyay, R. Investigation of the dynamical slowing down process in soft glassy colloidal suspensions: comparisons with supercooled liquids. *Soft Matter* **10**, 3292 (2014).
35. Ruzicka, B., Zulian, L. & Ruocco, G. Kinetics of the glass transition of fragile soft colloidal suspensions. *J. Phys.: Condens. Matter* **16**, S4993–S5002 (2004).
36. Saha, D., Joshi, Y. M. & Bandyopadhyay, R. Kinetics of the glass transition of fragile soft colloidal suspensions. *J. Chem. Phys.* **143**, 214901 (2015).
37. Jabbari-Farouji, S., Wegdam, G. H. & Bonn, D. Aging of rotational diffusion in colloidal gels and glasses. *Phys. Rev. E* **86**, 041401 (2012).
38. Jabbari-Farouji, S., Zargar, R., Wegdam, G. H. & Bonn, D. Dynamical heterogeneity in aging colloidal glasses of Laponite. *Soft Matter* **8**, 5507 (2012).
39. Maggi, C., Di Leonardo, R., Ruocco, G. & Dyre, J. C. Measurement of the Four-Point Susceptibility of an Out-of-Equilibrium Colloidal Solution of Nanoparticles Using Time-Resolved Light Scattering. *Phys. Rev. Lett.* **109**, 097401 (2012).
40. Berne, B. J. & Pecora, R. *Dynamic Light Scattering: With applications to Chemistry, Biology, and Physics.* John Wiley & Sons, New York (1975).
41. Pusey, P. N. In *Photon Correlation Spectroscopy and Velocimetry*, edited by Cummins, H. Z. & Pike, E. R. Plenum, New York (1977).
42. van Megen, W. *et al.* Measurement of the self-intermediate scattering function of suspensions of hard spherical particles near the glass transition. *Phys. Rev. E* **58**, 6073 (1998).
43. Cipelletti, L. & Ramos, L. Slow dynamics and internal stress relaxation in bundled cytoskeletal networks. *J. Phys.: Condens. Matter* **17**, R253–R285 (2005).
44. Ruzicka, B., Zulian, L. & Ruocco, G. Routes to Gelation in a Clay Suspension. *Phys. Rev. Lett.* **93**, 258301 (2004).
45. Ali, S. & Bandyopadhyay, R. Use of Ultrasound Attenuation Spectroscopy to Determine the Size Distribution of Clay Tactoids in Aqueous Suspensions. *Langmuir* **29**, 12663 (2013).
46. Lindsey, C. P. & Patterson, G. D. Detailed comparison of the Williams-Watts and Cole-Davidson functions. *J. Chem. Phys.* **73**, 3348 (1980).
47. Hunter, G. L. & Weeks, E. R. The physics of the colloidal glass transition. *Rep. Prog. Phys.* **75**, 066501 (2012).
48. Kroon, M., Wegdam, Gerard, H. & Sprik, R. Dynamic light scattering studies on the sol-gel transition of a suspension of anisotropic colloidal particles. *Phys. Rev. E* **54**, 6541 (1996).
49. Lacevic, N., Starr, F. W., Schroder, T. B. & Glotzer, S. C. Spatially heterogeneous dynamics investigated via a time-dependent four-point density correlation function. *J. Chem. Phys.* **119**, 7372 (2003).
50. Toninelli, C., Wyart, M., Berthier, L., Biroli, G. & Bouchaud, J.-P. Dynamical susceptibility of glass formers: Contrasting the predictions of theoretical scenarios. *Phys. Rev. E* **71**, 041505 (2005).
51. Nordstrom, K. N., Gollub, J. P. & Durian, D. J. Dynamical heterogeneity in soft-particle suspensions under shear. *Phys. Rev. E* **84**, 021403 (2011).
52. Berthier, L. *et al.* Spontaneous and induced dynamic fluctuations in glass formers. I. General results and dependence on ensemble and dynamics. *J. Chem. Phys.* **126**, 184503 (2007).
53. Berthier, L. *et al.* Spontaneous and induced dynamic correlations in glass formers. II. Model calculations and comparison to numerical simulations. *J. Chem. Phys.* **126**, 184504 (2007).

Acknowledgements

We acknowledge Department of Science and Technology, India for funding the research work.

Author Contributions

P.G. and R.B. conceived the experiments and directed the research. P.G. and S.K.B. conducted the experiments. Results are analysed and discussed by all the authors. P.G. has written the first draft of the manuscript. R.B. and D.S. provided revisions to the manuscript.

Additional Information

Supplementary information accompanies this paper at doi:10.1038/s41598-017-08495-9

Competing Interests: The authors declare that they have no competing interests.

Publisher's note: Springer Nature remains neutral with regard to jurisdictional claims in published maps and institutional affiliations.



Open Access This article is licensed under a Creative Commons Attribution 4.0 International License, which permits use, sharing, adaptation, distribution and reproduction in any medium or format, as long as you give appropriate credit to the original author(s) and the source, provide a link to the Creative Commons license, and indicate if changes were made. The images or other third party material in this article are included in the article's Creative Commons license, unless indicated otherwise in a credit line to the material. If material is not included in the article's Creative Commons license and your intended use is not permitted by statutory regulation or exceeds the permitted use, you will need to obtain permission directly from the copyright holder. To view a copy of this license, visit <http://creativecommons.org/licenses/by/4.0/>.

© The Author(s) 2017